Design and Analysis of Dual Output Flyback Converter for Standalone PV/Battery System

Jayalaksmi N. S. *‡, D. N. Gaonkar**, and Amrut Naik *

*Department of Electrical and Electronics Engineering, Manipal Institute of Technology, Manipal, India-576104
**Department of Electrical and Electronics Engineering, National Institute of Technology, Karnataka, Surathkal, India-575025

‡Corresponding Author; Jayalakshmi N. S., Department of Electrical and Electronics Engineering, Manipal Institute of Technology, Manipal, India-576104, Tel: +91-9481970925, jayalakshmi.ns@manipal.edu

Received: 20.12.2016 Accepted: 11.03.2017

Abstract - In this paper, the cost comparison is carried out among flyback, forward and full bridge converters based upon the number of circuit components. The performance assessment in terms of efficiency of the PV array with MPPT controller using flyback and forward converter is detailed. The design and control of Photovoltaic/battery system using a flyback converter for stand-alone applications is presented. A flyback converter is used to get DC output along with an AC output for high frequency applications without employing an inverter. The PV/battery system uses photovoltaic array as the main source of power and a battery as the storage device. The energy input of the PV system is effectively utilized by adopting an MPPT technique and the storage battery is controlled to balance the load requirements using a bi-directional dc-dc converter. This system ensures that the load demand is satisfied under varying solar irradiance conditions and a constant voltage is maintained for different load conditions. The modelling and control strategy of the implemented system is realized in MATLAB/Simulink environment.

Keywords **–**Flyback converter, cost analysis, PV system, MPPT controller, battery storage, battery controller

1. Introduction

The conventional energy sources are going to be exhausted in a few years. Hence we are in need of an infinite alternate energy source which can satisfy our demands effectively and efficiently. This leads us to the usage of renewable energy resources. One of the main renewable energy sources available in abundance is the solar energy. There is a huge support for generating electricity through solar energy as there is no carbon emissions related with them. Making the best use of solar energy depends on the efficiency and reliability of the technology involved. As the solar energy occurs at irregular intervals of time, utilizing this energy in a stand-alone system requires a corresponding storage capacity. There are many storage technologies including super capacitors, thermal storage, compressed air etc. The most cost effective and widely used technology is battery storage. Continuous supply of power is ensured by the combined operation of PV and battery storage system. In order to maximize this usage in our day-to-day life we must incorporate power electronic devices that can reliably control and convert the power according to the user needs. Thus for the successful operation of the PV system the interfacing of power electronic components play a major role. The DC – DC converters are needed in tracking the maximum power out of a PV energy source.

There are several DC - DC converters that are used in power electronic based applications. However, the DC - DC converters can be broadly classified as isolated and non-isolated converters. Every such converter will have its own advantage and disadvantage depending on the required application. In the present paper, the target application is solar-battery powered stand-alone system for rural applications. The converter should be able to provide two output ports for DC and AC loads with minimum circuit components. Depending upon the requirement of voltage levels between the input and output the choice of non-isolated DC- DC converters namely buck, boost, buck-boost, cuk or sepic is made. But in order to get an AC output from any of these converter topologies, an inverter is required which will increase the circuit complexity and number of components [1]. Also in the non-isolated converters there will be an electrical contact between the input and output part of the circuit. Because there is no isolation provided between the drive and power circuits, the converter is unsafe under fault conditions. Also one cannot easily get multiple power supplies out of a non-isolated converter and galvanic isolation cannot be provided between different output ports. Considering all these

factors the use of non – isolated converters for the target application is not found to be suitable. Isolated converters are a better choice when multiple isolated outputs are required.

A flyback converter operated under boost mode consists of less number of components then the conventional boost converter and also it can operate with a choke of low inductance value [2]. A flyback topology with a simple transformer structure along with a lossless snubber is an attractive choice for low power applications as they can be built with low cost and excellent efficiency [3]. A forward converter is a well – known and excellent topology when used in medium and low power applications. A forward converter is similar to a buck topology and can also step up the voltage depending on the turns ratio with no changes in the converter part [4]. By operating the forward converter under discontinuous conduction mode (DCM), better performances can be obtained with increased efficiency as the reverse recovery current of diodes is eliminated [5]. By giving suitable pulses to the switches of a full bridge DC – DC converter the impedance seen by the source is changed and maximum power tracking is achieved. This full bridge is converter is used to boost the output voltage of a PV panel and it is found to be efficient for the entire operating period [6]. As the converter uses four switches, the complexity of the drive circuit increases. Also the full bridge converter is mainly preferred for high power applications. A cost comparison between the three converters namely flyback, forward and full bridge converter is done [7] and a cost effective converter is chosen for the required application.

By employing an MPPT controller, a highly efficient system is obtained by delivering maximum power from the PV array to the load under varying irradiance and temperature conditions [8]. Flyback and forward converters are considered for the MPPT application and an efficient converter out of the two is chosen for the performance analysis of the PV/battery hybrid system. The controller for the battery is designed using a buck-boost bidirectional converter. With the help of this bidirectional converter, the battery can control the DC bus voltage constant irrespective of the changes in irradiance [9]. If the battery is directly connected across the load it cannot regulate the DC link voltage and in this method charge-discharge control cannot be achieved. So instead of connecting the battery directly across the load, the battery is connected to the DC link with another bidirectional dc-dc converter. The State of Charge (SOC) and V_{dc} limit ensures the safe operation of the battery and avoids unnecessary charge or discharge [10]. The rural areas where there is no supply of power or shortage of power and where people still use kerosene for lighting can use this present model which provides both DC and AC output.

In this paper, the cost comparison is carried out among flyback, forward and full bridge converters based upon the number of components. The performance assessment in terms of efficiency of the PV array with MPPT controller using flyback and forward converter is detailed. A dual output (DC and AC) flyback converter using a PV source as input is presented and its main application is electronic loads (DC) and rural lighting (AC). A battery with its controller for regulation of V_{dc} and SOC is presented which can charge and discharge and balance the load power under varying irradiance conditions. This system provides constant voltage at the output for different load conditions and provides a continuous supply of power to the load with the help of battery.

2. Cost Analysis and Performance of Converters

2.1 Cost analysis

A cost comparison analysis is made among flyback, forward and full bridge converters based upon the number of components [8] as shown in Table 1.

Table 1. Main converter components and corresponding cost

Components	Flyback Converter	Forward Converter	Full-bridge Converter
*Active switches	1 (Rs.30)	1 (Rs.30)	4 (Rs.120)
Gate driver IC	1 (Rs.60)	1 (Rs.60)	2 (Rs.120)
High frequency Diodes	1 (Rs.5)	2 (Rs.10)	4 (Rs.20)
**Isolation transformer	1 (Rs.300)	1 (Rs.350)	1 (Rs.300)
Filter inductor	1 (Rs.50)	1 (Rs.50)	1 (Rs.50)
Capacitor	1 (Rs.100)	2 (Rs.200)	2 (Rs.200)
Snubber	1 set (Rs.20)	1 set (Rs.20)	0
Total price	Rs.565	Rs.720	Rs.810

*All switches considered are of the same rating. Cost will change if the switches considered are of different rating.

**For all the converters, the transformer core chosen is same (its cost remains same) for given current rating.

After carrying out cost analysis, full bridge dc-dc converter is not considered due to the increased cost and complexity of triggering circuit. The flyback converter or forward converter are selected in this work owing to less number of components and lower price of the converters.

2.2 Performance of flyback and forward converter

The basic operation of the flyback converter is similar to that of a non-isolated buck-boost converter. The design of these two converters is made for the PV array parameters given in Table 3. The output voltage $\boldsymbol{V_o}$ required is 24 volts. The relation between input and output of the flyback converter is given by equation (1).

$$\frac{\boldsymbol{V_o}}{\boldsymbol{V_s}} = \frac{\boldsymbol{N_2}}{\boldsymbol{N_1}} * \left(\frac{\boldsymbol{D}}{\boldsymbol{1-D}}\right) \quad (1)$$

Initially the value of duty ratio (D) is assumed to be 0.4. Substituting this value in equation (1) we get, $\frac{\boldsymbol{N_2}}{\boldsymbol{N_1}} = 2.11$. Rounding the turns ratio to integer value, 2. Recalculating the duty ratio using equation (1), D = 0.4137.

Table 2. Efficiency of flyback and forward converter for PV array

Load resistance (Ohms)	Fly back converter			Forward converter		
	Solar input (W)	Load power (W)	Efficiency (%ge)	Solar input (W)	Load power (W)	Efficiency (%ge)
20	39.8	35.67	89.62	38.9	33.52	86.16
30	39.43	35.41	89.80	38.12	32.47	85.17
40	39.42	34.98	88.73	38.69	33.29	86.04

The magnetizing inductance current ($\boldsymbol{I_{LM}}$) is given by equation (2). Substituting the respective values in equation (2), the calculated value of $\boldsymbol{I_{LM}}$ is 2.7292A.

$$\boldsymbol{I_{LM}} = \frac{\boldsymbol{V_o}}{\boldsymbol{(1-D)R}} * \frac{\boldsymbol{N_2}}{\boldsymbol{N_1}} \quad (2)$$

The value of magnetizing inductance is given by equation (3). Here $\Delta\boldsymbol{I_{LM}}$ represents the peak-to-peak variation in the inductor current which is often used as a design criterion to determine the values of inductance. And the current variation in $\boldsymbol{L_m}$ is taken as 40 % of the average current: $\Delta\boldsymbol{I_{LM}}$ = 0.4 * 2.9292 = 1.08 A. Taking a switching frequency of 20 KHz, the value of $\boldsymbol{L_m}$ is calculated to be 332 µH.

$$\boldsymbol{L_m} = \frac{\boldsymbol{V_s D}}{\boldsymbol{\Delta I_{LM} f}} \quad (3)$$

The output ripple voltage of the converter is given by equation (4). The output voltage ripple ($\Delta\boldsymbol{V_o}$) is to be limited to 2 % of the output voltage, which is 0.02 *24 = 0.48 V. substituting these values in equation (4), the capacitance *C* is calculated to be 41 µF.

$$\frac{\Delta\boldsymbol{V_o}}{\boldsymbol{V_o}} = \left(\frac{\boldsymbol{D}}{\boldsymbol{RCf}}\right) \quad (4)$$

The forward converter is another magnetically coupled isolated topology. The transformer has three windings and the third winding is used to reduce the magnetizing current to zero before the start of every switching cycle. The relation between input and output voltage is given by equation (5).

Let the turns ratio $\left(\frac{\boldsymbol{N_3}}{\boldsymbol{N_1}}\right) = \boldsymbol{1}$. Initially taking a duty ratio of 0.4, the turns ratio is calculated to be $\frac{\boldsymbol{N_2}}{\boldsymbol{N_1}}$ = 3.

$$\frac{\boldsymbol{V_o}}{\boldsymbol{V_s}} = \boldsymbol{D}\left(\frac{\boldsymbol{N_2}}{\boldsymbol{N_1}}\right) \quad (5)$$

In forward converter $\boldsymbol{L_m}$ is not a parameter that is included in the input output relationship. And hence the value of magnetizing inductance is chosen as 332µH using equation (3). The value of output inductance $\boldsymbol{L_x}$ is determined using equation (6) which is the inductor current equation when the switch is open. $\Delta\boldsymbol{I_{Lx}}$ is calculated to be 0.4A and the value of $\boldsymbol{L_x}$ is calculated to be 1.5mH.

$$\boldsymbol{L_x} = \frac{\boldsymbol{V_o(1-D)}}{\boldsymbol{\Delta I_{Lx} f}} \quad (6)$$

The output voltage ripple of the converter is given by equation (7). Taking 2 % ripple in the output voltage which is 0.02 *24 = 0.48 V, the value of capacitance is calculated to be 5.2µF using equation (7).

$$\frac{\Delta\boldsymbol{V_o}}{\boldsymbol{V_o}} = \frac{\boldsymbol{1-D}}{\boldsymbol{8LCf_s^2}} \quad (7)$$

The performance assessment in terms of efficiency of the PV array with MPPT controller using flyback and forward converter is detailed in Table 2.

From the comparison given in Table 2, it is realized that even though both flyback converter and forward converter topologies employ only one switch, efficiency of flyback converter is more compared to a forward converter. In addition the forward converter requires an extra demagnetizing winding which increases the cost. Hence, in this work a flyback converter is chosen to analysis the performance of a PV/battery system.

3. Configuration of the System

Figure 1 depicts the block diagram representation of the PV/battery system using dual output flyback converter. The PV system consists of four PV arrays each of 10 W which are connected in series. The PV panel is connected to the load through the flyback converter. The load consists of both DC and AC loads on the secondary side of the flyback transformer. The maximum power point tracking algorithm ensures that maximum power from the PV module is delivered to the load, which is facilitated by the adjustment of duty cycle of the converter. The PV panel and battery act as central system and charge-discharge system respectively.

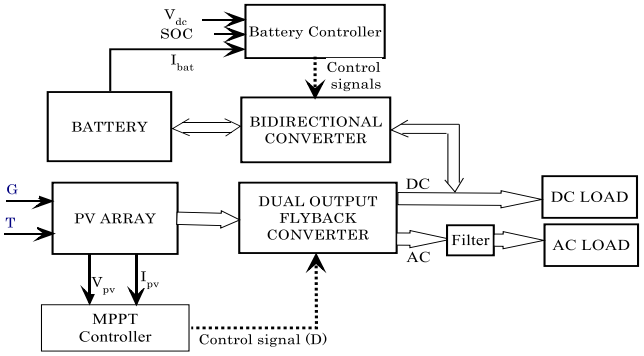

Fig. 1 Block diagram representation of the PV/battery system

4. System Modelling

4.1 Modeling of PV array and MPPT Controller

The detailed modeling of PV array is reported in [11]. The single diode model of solar cell is the simplest and commonly used model whose equivalent circuit is as shown in Figure 2.

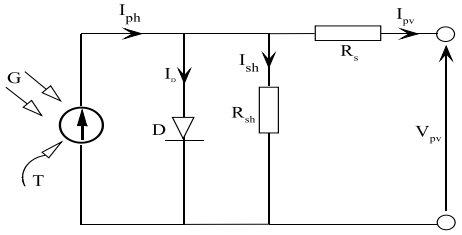

Fig. 2 Electrical equivalent circuit of a PV cell

The photocurrent I_{Ph} produced by the sunlight is represented by a current source and by applying KCL to the circuit in Figure 2 is given by equation (8).

$$I_{pv} = I_{ph} - I_D \tag{8}$$

Where, I_D is the diode internal diffusion current. R_{sh} *and* R_s are diode internal shunt and series resistance. The output voltage and current of the PV cell is given as V_{PV} *and* I_{PV} respectively. The current I_D is given by equation (9).

$$I_D = Is\left[e^{\left(\frac{qVpv}{AKTc}\right)} - 1\right] \tag{9}$$

Where, A is the diode ideality factor, K is the Boltzmann's constant, q is the charge of electron and T_C is operating temperature. The diode saturation current is given by the expression is given by equation (10).

$$I_S = I_{RS}\left(\frac{T_C}{T_{Ref}}\right)^3 exp\left[\frac{qE_{gap}}{AK}\left(\frac{1}{T_{Ref}} - \frac{1}{T_C}\right)\right] \tag{10}$$

T_{Ref} is the reference cell temperature in Kelvin (K). E_{gap} is the semiconductor band-gap energy of the PV cell. I_{RS} is the reverse saturation current of the PV cell in ampere (A) at the standard temperature. The photocurrent I_{Ph} is defined as

$$I_{Ph} = \left[I_{SC} + K_I\left(T_C - T_{Ref}\right)\right] * \frac{G}{1000} \tag{11}$$

Where, I_{SC} is the short circuit current at standard temperature 25℃ and solar irradiation of 1000 W/m^2. The expression for PV array output current is given by equation (12).

$$I_{PV} = I_{Ph} - I_S \times \left[exp\left(\frac{q\times(V_{PV}+I_{PV}\times R_S)}{A\times K\times T_C}\right) - 1\right] \tag{12}$$

The flowchart for P and O algorithm is depicted in Figure 3.

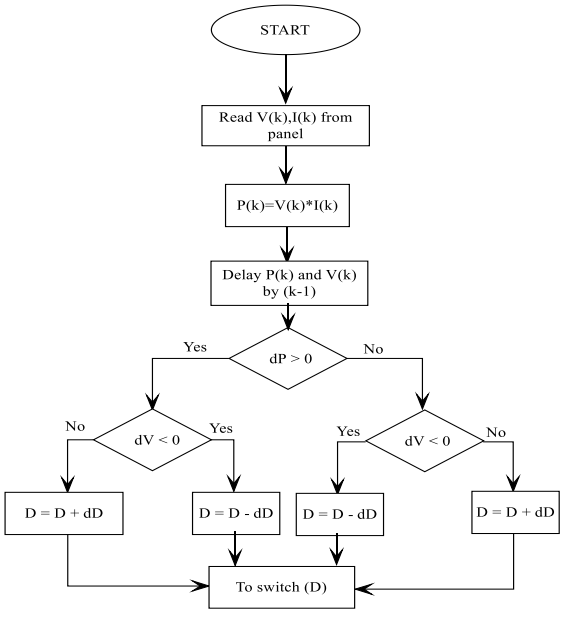

Fig. 3 P and O algorithm flowchart

The MPPT methods that are available ranges from simple relationships between current and voltage to complex algorithms. These include constant voltage method, fractional open circuit voltage or short circuit current algorithm, perturb and observe (P and O) method, incremental conductance method and temperature based control method [12]. However owing to the simplicity involved in the design and implementation of P and O algorithm in low power applications along with good performance makes it one of the most widely used MPPT techniques for solar PV applications [13, 14]. Hence the same MPPT technique has been used in the present model for the PV/battery system. This algorithm is based on current and voltage sensing to track MPP. The system is perturbed in one direction and if the power continues to increase then the algorithm should keep perturbing in the same direction. If the power calculated is less than the previous calculated power then the perturbation is done in the opposite direction. These steps are continued till the maximum power point is reached.

4.2 Modeling of Flyback converter

The circuit diagram of the flyback converter used in this system is represented in Figure 4. A dual output flyback topology providing a regular DC output along with a high frequency AC output is shown to be efficient when compared to a converter where dc-dc-ac conversion is cascaded as the switching losses associated with the later approach is comparatively more [15]. This model employs a single DC source as the input, which can be replaced by a solar photovoltaic source along with a storage battery for rural based applications. Also this model makes use of a PWM controller instead of MPPT technique which is not as efficient as the later.

The discontinuous conduction mode (DCM) operation is preferred for low current and high voltage applications and continuous conduction mode (CCM) of operation is preferred for high current and low voltage applications [16]. In spite of disadvantages offered by DCM mode of operation of flyback converters over CCM mode, the DCM mode of operation is preferred because of fast response to load current and input voltage variations [17]. The flyback converter is a suitable converter for high frequency, with low power applications [18]. The present model is developed for the rural applications where DC for battery charging or other electronic loads and AC can be used for high frequency loads such as lighting.

A flyback converter topology is basically buck - boost topology that is isolated by using a transformer. Though the three winding magnetic device is named as a transformer, the more accurate name for that would be a three winding split inductor. To obtain a positive output, polarity marks are reversed and the current cannot flow in both the windings of flyback transformer simultaneously unlike the ideal transformer. This flyback topology proposed here is similar to the conventional topology except for the fact that it has an additional output port for providing the required AC output.

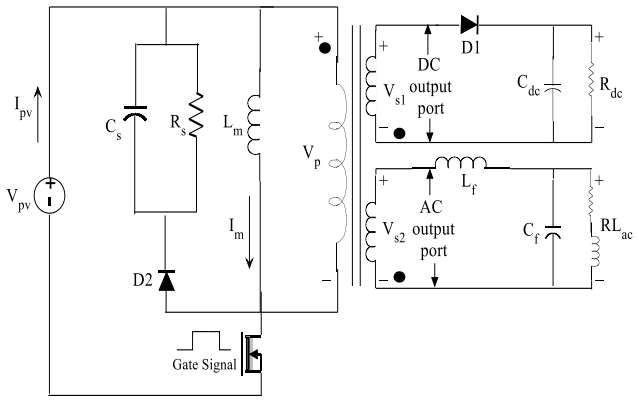

Fig. 4 Circuit diagram of flyback converter

The flyback converter has three operating modes based on the ON and OFF switching period under discontinuous conduction mode. In the first mode, when the switch is turned ON, the voltage V_{in} is applied to the primary of the transformer. The inductor stores energy and on the secondary DC side the diode acts an open circuit due to reverse polarity and load is supplied by the output capacitor. So when the primary conducts the secondary remains isolated and does not conduct. In the second mode, when the switch is closed, the diode connected in series with the secondary winding starts to conduct as the voltage polarities are reversed. The current in the transformer magnetizing inductance decreases to zero before the start of the next cycle. In the third mode, the secondary winding Electromotive force (emf) and current fall to zero. The diode connected in series with the secondary winding stops conducting after the stored magnetic field energy has been completely transferred to the output. However the load voltage is supplied by the output capacitor and the discontinuous mode ends when the switch is turned on. And the sequence repeats again. The equations (13) and (14) are used for the design of DCM mode of flyback converters.

$$Vin = L_m \frac{diLm}{dt} = L_m \frac{\Delta iLm}{DT} \tag{13}$$

$$I_{Lm,max} = \frac{VpvDT}{Lm} \tag{14}$$

The output voltage for discontinuous operation can be determined by analysing the power equations of the input and output. Assuming ideal components, the power supplied by the input source is the same as the power supplied by the load resistor. By equating the input and output power as shown in the equations (15) and (16)

$$Ps = Po \tag{15}$$

$$Vpv * Ipv = \frac{Vo^2}{R} \tag{16}$$

Average source current is the area under the triangular waveform and is given by following equations,

$$Is = \frac{1}{2} * \frac{VpvDT}{Lm} * DT * \frac{1}{T} = \frac{VpvD^2T}{2Lm} \tag{17}$$

$$\frac{VpvD^2T}{2Lm} = \frac{Vo^2}{R} \tag{18}$$

The designed value of Lm is 600µH.

The parallel combination of capacitor C_s and resistor R_s along with a series diode represents the snubber circuit. The snubber diode provides a low impedance path for the primary winding leakage inductance current into the snubber capacitor. The resistor connected in parallel with the capacitor avoids any excess build-up of voltage across it. The proper values should be chosen for the snubber resistor and capacitor to make sure that no part of the energy stored in the mutual flux of the windings is taken by the capacitor. And this is achieved by keeping the RC time constant of the snubber circuit relatively more than the switching time of the converter which is given by equation (19). The values of R and C are 3.9 KΩ and 68nF respectively.

$$RC > T \text{ or } RC > 1/20Khz \tag{19}$$

5. Battery Controller

The battery controller can regulate the voltage of a DC bus despite of sudden irradiance changes. It is seen that PV and battery can transfer power to the output simultaneously and it is an effective system for powering dynamic loads such as solar cars, domestic loads and back-up systems [19-21]. The circuit diagram of a bidirectional converter is shown in Figure 5. To enable the proper battery charging and discharging through the bidirectional converter a control scheme is employed as shown in Figure 6. The primary objective of the controller is to maintain the dc link voltage constant along with keeping SOC within safe limits.

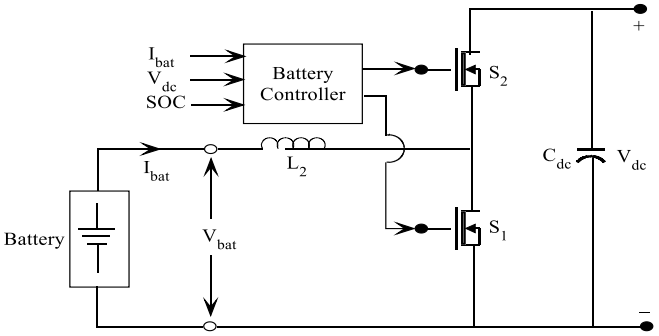

Fig. 5 Bidirectional converter

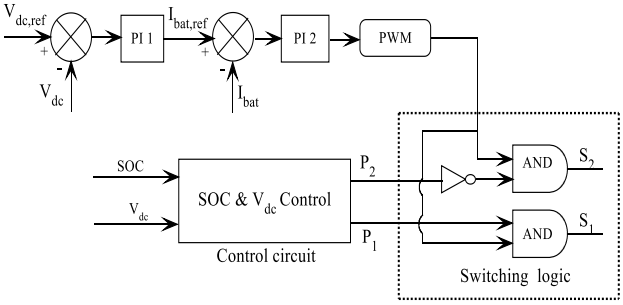

Fig. 6 Control scheme for Bidirectional converter

The DC bus voltage is maintained at a constant value of 24 volts ($V_{dc,ref}$). For this purpose a PI controller (PI1) with gains K_{p1} = 5 and K_{i1} = 0.12 is used. Also for controlling the battery current an internal PI controller with (PI2) is employed with gains K_{p2} = 5 and K_{i2} = 0.8. The output of the controller is given to the pulse generation circuit which triggers the switches S_1 and S_2 of the bidirectional converter in accordance with the SOC and Vdc control logic. The logic circuit decides the mode of operation of the battery which is shown in Figure 7 and thereby three modes of operation can be seen namely boost mode, buck mode and halt mode. These three modes of operation are considered under loaded condition. During the boost mode the switch S_1 is closed and S_2 is open. Hence the battery is in discharging state when the solar irradiation is less and solar power is not sufficient enough to supply the load. During buck mode the switch S_1 is open and S_2 is closed and the battery gets charged due to excess generation of solar power. In the halt mode of operation both the switches are open and no power is transferred to the load from battery. And if none of the loads are connected the bidirectional converter is disconnected from the system and the battery is allowed to charge.

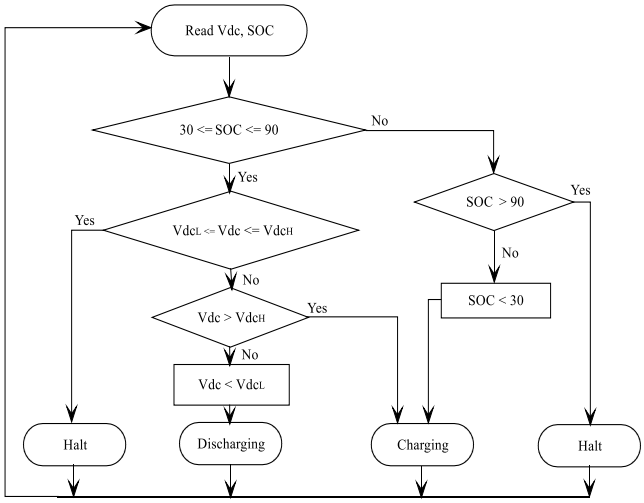

Fig. 7 Flowchart of SOC and charge controller

The algorithm developed for SOC and charge controller ensures the safe and optimal operation of the battery. The SOC upper limit is kept at 90 % while the lower limit is kept at 30 % only in order to avoid deep discharging of the battery. Also limit has been considered for V_{dc} to prevent unnecessary charging or discharging of the battery. The battery will charge or discharge only when the V_{dc} voltage deviate from the set limit (between 23.8 to 24.2V). This control circuit provides input for the switching logic and thereby triggers the corresponding switches. Switching pulses S_2 and S_1 are given to the bidirectional converter as input and P_1 and P_2 are the outputs of logic circuit.

6. Simulation Results

In this section, the simulation results of the PV/battery system are presented. The simulation study has been carried out for a period of 20 sec. For the analysis of the system, both DC (resistor) and AC loads (resistor-inductor) are considered. The system has been modeled and simulated using Simulink/MATLAB software. The simulation parameters of the PV cell and battery are given in Table 3. The PV model is implemented as an M-File code and it is electrically build as a voltage controlled current source with temperature, irradiation and PV voltage as inputs and current produced by the panel as the output parameter. For the performance analysis of the system four different cases are considered.

Table 3. Simulation parameters of the PV/battery system

Simulation parameters	Values
Maximum Power	10 W
Number of panels	4
Voltage at P_{max}	17 V
Current at P_{max}	0.59 A
V_{oc}	21 V
I_{sc}	0.62 A
Temperature	25 C
Irradiance	1000 W/m^2
Number of cells	36
Battery operating voltage	12 V
Ampere-Hour rating	20 AH (Lead-Acid)

Case 1: Effect of irradiation and temperature

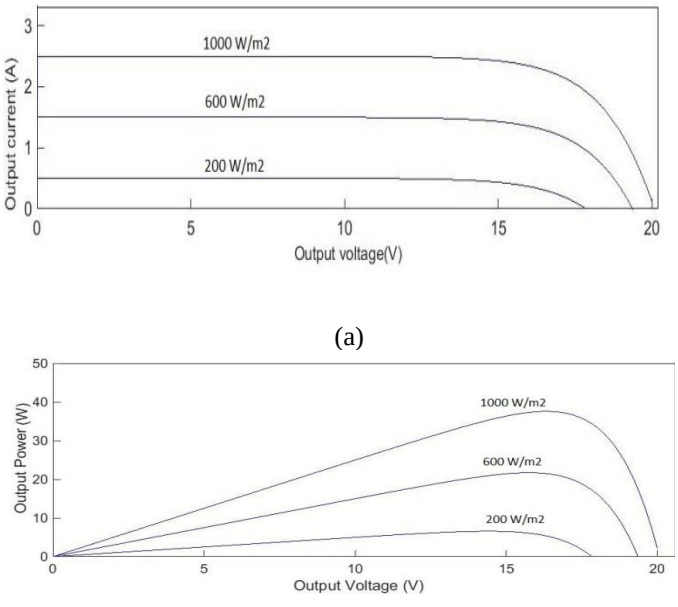

(a)

(b)

Fig. 8 The effects of irradiance on solar panel a) Effect of irradiance on the I-V characteristic b) Effect of irradiance on the P-V characteristic.

The open circuit voltage is highly influenced by the increase in the panel temperature. For constant irradiation, there will be a slight increase in the short circuit current because the band energy gap decreases and more photons have energy to create electron-hole pairs. But due to the drop in the open circuit voltage with the increase in temperature, there will be a decrease in the PV output power. The effect of temperature is shown in Figure 9.

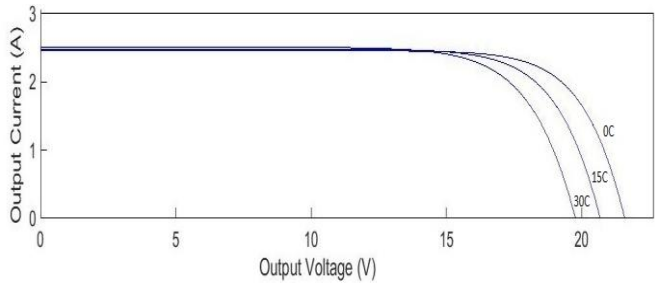

(a)

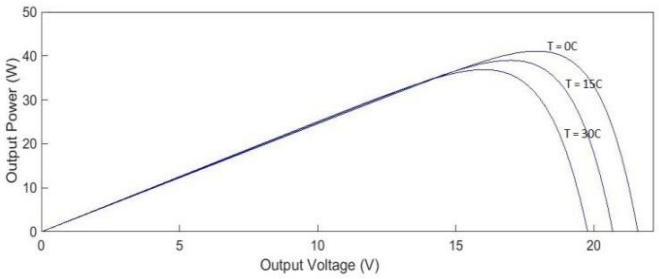

(b)

Fig. 9 The effects of temperature on solar panel a) Effect of temperature on the I-V characteristic b) Effect of temperature on the P-V characteristic

Case 2: Flyback converter operation under discontinuous flux mode

Figures in 10 shows current and voltage waveforms when the circuit is operating in DCM mode. During mode 3, the primary current, secondary current and the primary voltage is zero. But the load gets a steady voltage during this mode owing to high value of capacitor. Thus the output load voltage is kept constant during all the three modes of DCM.

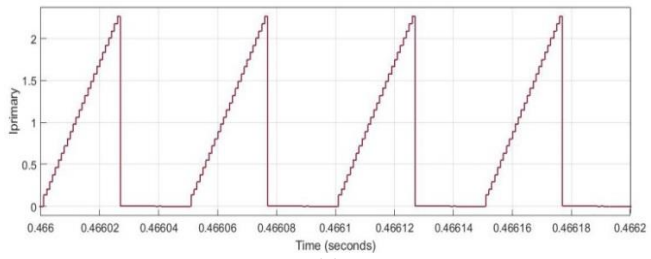

(a)

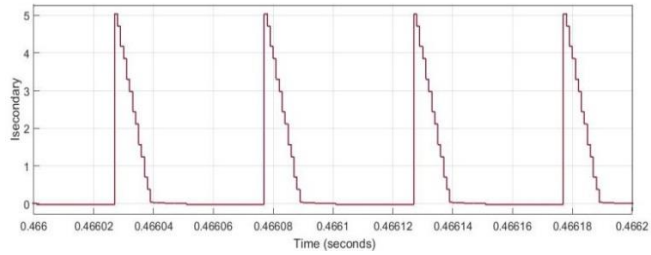

(b)

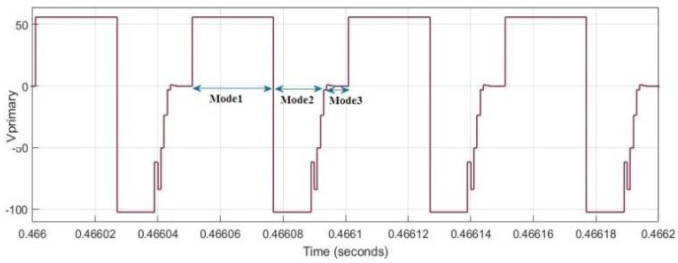

(c)

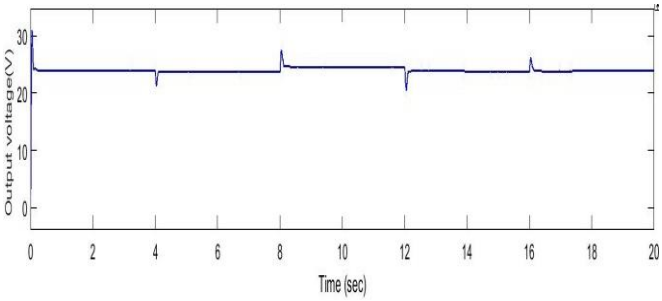

(d)

Fig. 10 Flyback converter operation under discontinuous flux mode a) Primary current of the Flyback converter b) Secondary current of the Flyback converter c) Primary voltage of the Flyback converter d) Output voltage of the Flyback converter.

Case 3: Performance study with variable irradiance condition

During the simulation, the irradiance is made to change at intervals of 4 seconds each as depicted in Figure 11 and the load demand is kept at 20W. At 4 second there is a decrease in solar irradiation, the PV power drops to 3W, and the battery is able to supply 17W to satisfy the load demand as shown in Figure 12. Also at 8 second when the PV power is greater then the demand, the battery stores the surplus power produced by the PV system as in Figure 12. The simulation results for power balancing between PV and battery under varying irradiance conditions is depicted in Figure 13.

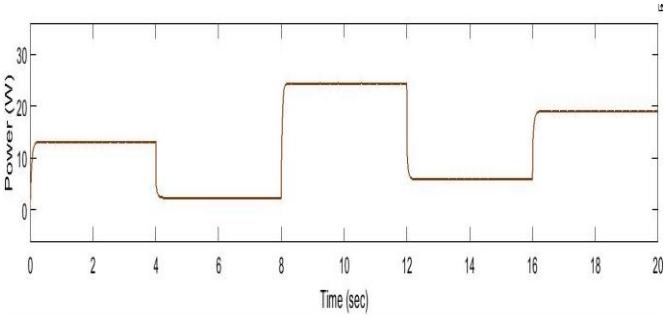

Fig. 11 Solar power variation

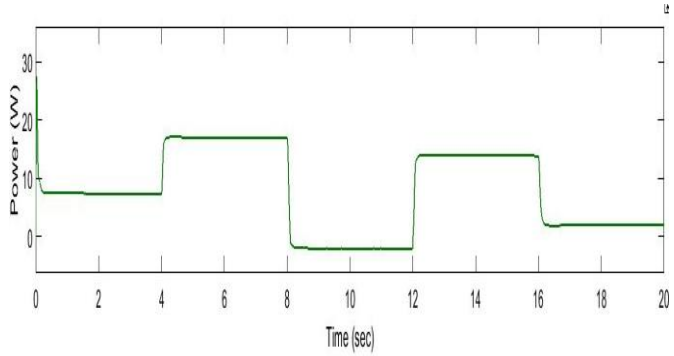

Fig. 12 Battery power

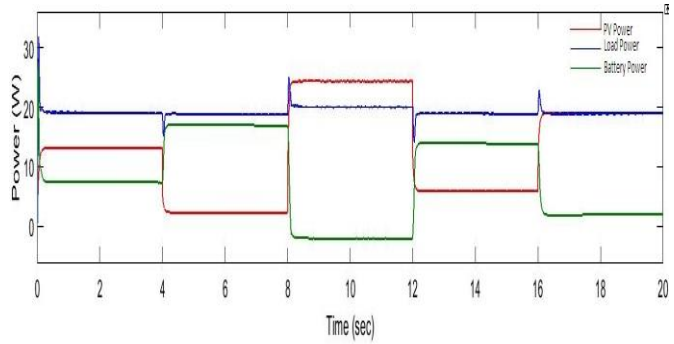

Fig. 13 PV power, battery and load power

Figure 14 and 15 shows the output waveforms of AC voltage and current. The total harmonic distortion (THD) of the AC output voltage is 4.72 % as shown in Figure 16.

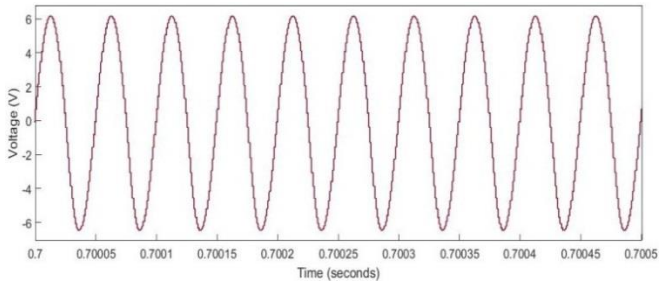

Fig. 14 Waveform of AC load voltage

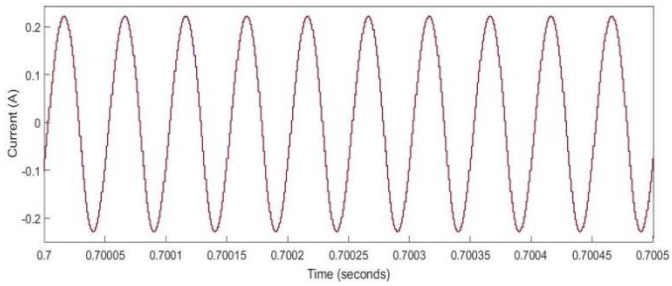

Fig. 15 Waveform of AC load current

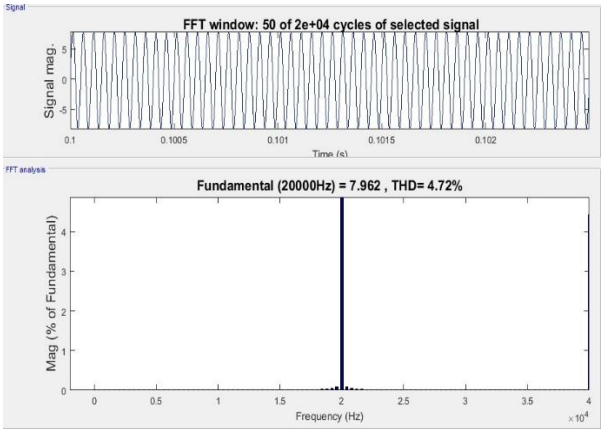

Fig. 16 THD of AC output voltage

Case 4: System performance for different loads

In Table 2 and 3 the performance of the system for different loads are considered. The irradiation is considered to be constant at 700W/m^2 and temperature of 25ºC. It is seen that according to the variations in the load resistance the output power changes and the battery supplies/stores the excess/deficit of PV power produced. The load power is considered to vary from 20W to 30W only as the system may go into non-linear region/flyback transformer may saturate for rapid load changes. In Table 4 the RL load is held constant at 25Ω and 100µH and the DC load is varied. In Table 5, the RL load is held constant at 30Ω and 200µH and the DC load is varied. It can be seen that for variations in the load, the DC output voltage remains constant. And the required AC/DC output power can be obtained by suitably adjusting the secondary number of turns of the flyback transformer.

Table 4: DC load variation with R_{ac} = 25Ω and 100µH.

DC load (ohms)	P_{pv} (W)	P_{load} (W) (P_{ac}+P_{dc})	$P_{battery}$(W)	V_{dc} (V)
15	19.89	39.12	21.11	23.92
20	19.89	29.87	11.76	23.98
25	19.88	24.35	6.25	24.01
30	19.87	20.53	2.447	24.02
35	19.83	17.95	-0.8125	24.10
40	19.88	15.86	-2.289	24.12

Table 5: DC load variation with R_{ac} = 30Ω and 200µH.

DC load (ohms)	P_{pv} (W)	P_{load} (W) (P_{ac}+P_{dc})	$P_{battery}$(W)	V_{dc} (V)
15	19.34	39.28	21.66	23.96
20	19.34	30.21	12.55	24.02
25	19.33	24.32	6.671	23.96
30	19.33	20.53	2.881	23.96
35	19.33	17.78	0.1708	23.98
40	19.32	15.92	-1.708	24.1

7. Conclusion

In this paper, the cost comparison among flyback, forward and full bridge converters based upon the number of circuit components is carried out with performance assessment of the PV array with MPPT controller using flyback and forward converter is detailed. For PV/battery system presented, a dual output flyback converter is chosen. The target application of this model is for rural lighting (AC loads) and other DC loads. The power balance is achieved with the help of battery controller under varying irradiance conditions. The flyback converter switching operation is controlled by MPPT controller. The battery is connected using bidirectional converter. The SOC of battery and DC voltage are regulated using battery controller. Also it is seen that for different load conditions the output voltage remains constant. It can be seen from the simulation results of the PV/battery system that the flyback converter is made to work under DCM mode of operation. The total harmonic distortion (THD) of the AC output voltage is 4.72 %.

References

[1] Dipankar Debnath, Kishore Chatterjee, "Solar photovoltaic-based stand-alone scheme incorporating a new boost inverter", IET Power Electronics, 2016, pp. 1-10.

[2] Adam Kawa, Adam Penczek, Stanislaw Pirog, "DC-DC boost-flyback converter functioning as input stage for one phase low power grid-connected inverter", Archieves of electrical engineering, VOL. 63(3), pp. 393-407 (2014).

[3] Siyang Zhao, Junming Zhang, Yang Shi, "A Low cost, low power flyback converter with a simple transformer", 2012 IEEE 7th International Power Electronics and Motion Control Conference - ECCE Asia, June 2-5, 2012, Harbin, China.

[4] McFowland, Nickolas Arthur, "Forward converter for solar power applications", (2012).*Masters Theses.*

[5] Jong-Hyun Lee, Do-Hyun Kim, Sol Mun, Minh Thao Nguyen, Viet Thang Tran, and Joung-Hu Park, " Series connected forward flyback converter for gigh step-up power application", 8th International Conference on Power Electronics - ECCE Asia, May 30-June 3, 2011, The Shilla Jeju, Korea.

[6] Calebe A. Matias1, Wesley P. Calixto, "Simulation and analysis of an isolated full-bridge DC/DC boost converter operating with a modified perturb and observe maximum power point tracking algorithm", 2016 IEEE 16th International Conference on Environment and Electrical Engineering (EEEIC).

[7] Hua Bai, Chris Mi, "Comparison and evaluation of different DC/DC topologies for plug-in hybrid electric vehicle chargers", Int. J. Power Electronics, Vol. 4, No. 2, 2012.

[8] João H. de Oliveira, Luan P. Carlette3, Allan F. Cupertino, Victor F. Mendes , Wallace do C. Boaventura and Heverton A. Pereira, "Comparison of MPPT Strategies in Battery Charging of Photovoltaic Systems"

[9] Hisham Mahmood, Student Member, IEEE, Dennis Michaelson, Member, IEEE,and Jin Jiang, Senior Member, IEEE, "A Power Management Strategy for PV/Battery Hybrid Systems in Islanded Microgrids," IEEE journal of emerging and selected topics in power electronics, VOL. 2, NO. 4, DECEMBER 2014.

[10] M. Z. Daud, A.Mohamed, M. Z. Che Wanik and M. A. Hannan, "Performance evaluation of grid connected system with battery energy storage," 2012 IEEE International conference on Power and Energy (PECON), 2-5 December 2012, Kota Kinabalu Sabah, Malaysia.

[11] Habbati Bellia, Ramdani Youcef, Moulay Fatima, "A detailed modelling of photovoltaic module using matlab," pp. 1-5, 2014.

[12] D. Freeman, "Introduction to photovoltaic systems maximum power tracking," Texas instruments Rapport D'application, SLVA-446 November, vol.2010, 2010.

[13] T. Esram and P. L. Chapman, "Comparision of photovoltaic array maximum power tracking technique," IEEE Transcations on Energy Conservation, vol. 22, p. 439, 2007.

[14] S. Jain and V. Agarwal, "Comparision of the performance of maximum power point tracking schemes applied to single stage grid connected photovoltaic systems," IET Electric Power Applications, vol.1, pp. 753-762, 2007.

[15] Luocheng Wang and Ali M. Bazzi, "A Dual AC and Dc output flyback converter," Workshop on control and modelling for power electronics (COMPEL), USA.

[16] Ashraf A. Mohammed and Samah M. Nafie, "Flyback converter design for low power application," International Conference on Computing, Control, Networking, Electronics and Embedded Systems Engineering, 2015, Khartoum, Sudan.

[17] Nasir Coruh, Satilmus Urgan and Tarik Erfidan "Design and Implementation of flyback converters," Kocaeli University, turkey, 978-1-4244-5046-6/10/$26.00c 2010 IEEE.

[18] Sanjeev Kumra Pandey, Dr. S. L. Patil and Mrs. Vijaya S. Rajguru, "Isolated flyback converter designing, modelling and suitable control strategies," Proc.of.Int.Conf.on Advances in Power electronics and Instrumentation engineering, PEIE.

[19] Chan H L, Sutanto D, "A new battery model for use with battery energy storage systems and electric vehicles power systems", Power Engineering Society Winter Meeting, pp. 470-475,2000.

[20] Jayalakshmi, N. S. and Gaonkar, D. N. (2015). "An integrated Control Approach and Power Management of Standalone Hybrid Wind/PV/Battery Power Generation System with Maximum Power Extraction Capability." *Distributed Generation and Alternative Energy Journal*, Taylor and Francis Publishers, U.K., 30(4), 15-36.

[21] Hsein K H. Muta L Joshino T. et al. "Maximum photovotaic power tracking: an algorithm for rapidly changing atmospheric conditions, generation, transmission and distribution", lEE Proceedings, Vol 142, No. 1, pp. 59-64, 1995.